Open Research Online

The Open University's repository of research publications
and other research outputs

Mapping radiation-induced defects in CCDs through space and time

Conference or Workshop Item

oro.open.ac.uk

Mapping radiation-induced defects in CCDs through space and time

David Hall[*], Nathan Bush, Daniel Wood, Neil J. Murray[†], Jason Gow,
Jesper Skottfelt and Andrew Holland

Centre for Electronic Imaging, DPS, The Open University, Milton Keynes, MK7 6AA, UK

ABSTRACT

The Charge Coupled Device (CCD) has long been the detector of choice for many space-based applications. The CCD converts the signal X-rays or visible light into electrons (n-channel devices) or holes (p-channel devices) which are stored in the pixel structure during integration until the subsequent transfer of the charge packets through the device to be read out. The transfer of this signal charge is, however, not a perfect process.

Throughout the lifetime of a space-based mission the detector will be bombarded by high-energy particles and gamma rays. As time progresses, the radiation will damage the detectors, causing the Charge Transfer Efficiency (CTE) to decrease due to the creation of defects or "traps" in the silicon lattice of the detector. The defects create additional energy levels between the valence and conduction band in the silicon of the detector. Electrons or holes (for n-channel or p-channel devices respectively) that pass over the defect sites may be trapped. The trapped electrons or holes will later be emitted from the traps, subject to an emission-time constant related to the energy level of the associated defect. The capture and emission of charge from the signal leads to a characteristic trailing or "smearing" of images that must be corrected to enable the science goals of a mission to be met.

Over the past few years, great strides have been taken in the development of the pocket-pumping (or strictly-speaking "trap pumping") technique. This technique not only allows individual defects (or traps) within the device to be located to the sub-pixel level, but it enables the investigation of the trap parameters such as the emission time constant to new levels of accuracy. Recent publications have shown the power of this technique in characterising a variety of different defects in both n- and p-channel devices and the potential for use in correction techniques, however, we are now exploring not only the trap locations and properties but the life cycle of these traps through time after irradiation. In orbit, most devices will be operating cold to suppress dark current and the devices are therefore cold whilst undergoing damage from the radiation environment. The mobility of defects varies as a function of temperature such that the mix of defects present following a cryogenic irradiation may vary significantly from that found following a room temperature irradiation or after annealing. It is therefore essential to study the trap formation and migration in orbit-like conditions and over longer timescales.

In this paper we present a selection of the latest methods and results in the trap pumping of n- and p-channel devices and demonstrate how this technique now allows us to map radiation-induced defects in CCDs through both space and time.

Keywords: CCD, Radiation Damage, Defects, Traps, Silicon, Pocket pumping, Trap pumping

1. INTRODUCTION

Charge Coupled Devices (CCDs) have been successfully used on many space missions over recent decades, from ESA's XMM-Newton [1] to Gaia [2,3]. Upcoming missions, such as ESA's Euclid [4-7], will make use of CCDs in their focal planes. Despite their excellent performance in terms of low noise and high quantum efficiency, the silicon in the CCDs is susceptible to damage from the often harsh radiation environment in space [8,9].

In order to minimise the impact of the damage caused by radiation whilst in-orbit, one can optimise the detector performance against the impact of the damage. Pre-launch testing of the devices allows the optimal conditions to be

[*] Corresponding author: david.hall@open.ac.uk; phone +44 (0)1908 659 579; www.open.ac.uk/science/research/cei

[†] Neil Murray now at Dynamic Imaging Analytics Limited, Bletchley Park Science & Innovation Centre, MK3 6EB, UK.

selected to minimise the impact of the radiation. However, the impact of the radiation damage may not be completely removed through optimisation alone and the remaining effects must be removed in software.

To correct the remaining radiation damage in software, one can make use of a charge transfer model that allows the simulation of the ideal signal passing through a damaged device. For Gaia, an analytical Charge Distortion Model (CDM) [10] is being used which is fitted to data to obtain the required parameters for the simulation. For Euclid, a forward modelling approach is being used through a semi-empirical form of model (combining analytical and Monte Carlo elements), similar to that used for the Hubble Space Telescope [11]. Regardless of the model type, the simulations carried out are only as good as the parameters used.

Over the last few years, developments in the technique of "pocket pumping" [12] have allowed the analysis of defects (or traps) in the silicon lattice to new levels of accuracy and depth. The use of the technique for Gaia enabled the more detailed study of the capacity of the supplementary buried channel, such as is detailed in [13], whilst the tracking of the efficiency of trapping with temperature allowed the study of traps in more detail in p-channel CCDs [14]. Further study of the technique and the impact of varying clocking sequences and temperatures of operation has allowed more in depth and detailed optimisation of CCDs [15,16], with a more detailed understanding of the traps present allowing simulations to drive further clocking optimisation [17]. By studying individual traps in single pixels in the CCD, a process commonly referred to as "trap pumping" due to the study of "traps" primarily instead of potential "pockets", one can allow more in depth optimisation of the CCD operation and allow more accurate parameterisation for charge transfer simulation. Furthermore, through the variation of both temperature and clock timings at a constant phase-to-phase frequency, the resonance of the trap emission can be probed to allow the parameters of each single trap to be measured to within a few percent accuracy [18-20].

Through the technique of trap pumping, one can locate each single trap within the CCD with sub-pixel accuracy. In some devices, depending on the number of phases and any additional doping present, it is possible to find the trap location to the sub-electrode level (i.e. within a few microns) as well as estimating the trap depth through adjusting the background level and applied voltages. Perhaps even more useful is the ability to track traps from irradiation, through annealing and further transitions in the device. Different irradiation conditions can be studied in intense detail and the impact and importance of cryogenic irradiations has been strongly demonstrated [21-23]. The technique is being used as a tool to understand the impact of radiation damage on CCDs for future mission studies, such as in the low-signal regime for WFIRST [24-27].

Beyond the clear advantages of understanding defect formation and annealing within devices, the results from trap pumping in CCDs can direct the production of charge transfer models. Parameters determined through trap pumping can be input directly into charge transfer models to provide a highly physical simulation of charge transfer in a radiation damaged CCD, offering the potential for improved correction techniques. Here we present a review of the technique and a selection of the latest results that demonstrate its use and the potential use in future applications. Specific details of the irradiations and devices are not included as the intention is to demonstrate the technique and not to lose this within the detail of specific irradiation campaigns.

2. RADIATION DAMAGE TO THE SILICON LATTICE

When placed in space, the silicon in the CCD is constantly being bombarded by high energy particles and gamma-rays, some passing through the spacecraft and some as secondaries from the shielding materials surrounding the detectors. The spectrum of particles incident on the spacecraft varies with orbit, from the domination of electrons for ESA's JUICE mission to the protons that will dominate for Euclid. Whilst there are a variety of damage mechanisms [28], in this paper we are concentrating on displacement damage and the silicon lattice defects (or traps) created.

When high energy protons pass through the detector, they effectively knock silicon atoms from their uniform lattice positions, Figure 1. The absence of a silicon atom (a vacancy) will diffuse through the lattice until it forms a stable defect such as a divacancy (pairing with another vacancy) or with a dopant or impurity atom, such as with oxygen for the Si-A or phosphorous for the Si-E.
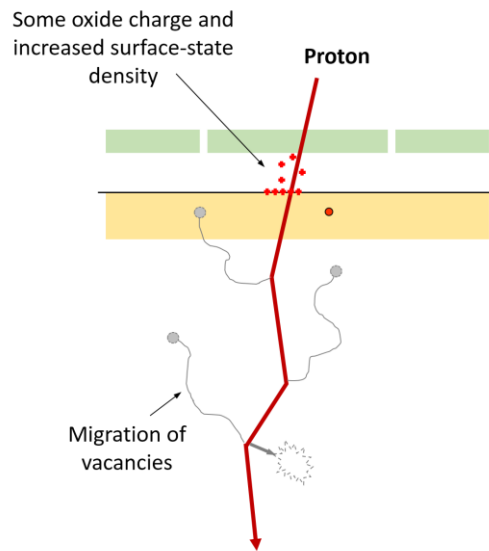
Figure 1. When in space, the detectors are bombarded by high energy protons. These protons effectively "knock" silicon atoms from the lattice, creating vacancies that will migrate until they form a stable lattice defect. An energy level is formed between the valence and conduction bands in the silicon that acts to trap passing signal charge carriers (electrons or holes), releasing these at a later point in time subject to the related emission time constant. Figure adapted from the diagrams of David Burt.

3. LATTICE DEFECTS AND TRAPS

The diffusion of vacancies through the lattice allows the creation of a variety of different stable defect (trap) structures. The mobility and stability of different species of traps varies with temperature; some defect species are frozen out at low temperatures and only become mobile at higher temperatures. As such, the population of traps will vary as a function of temperature and time.

Each trap can be described with an energy level between the valence and conduction bands in the silicon band structure. The energy level of the trap impacts the dynamics of the trap, with the emission time constant dependent on the energy level in question. As signal charge (electrons/holes in n-channel/p-channel devices respectively) interacts with the traps as it is transferred through the device, the traps can capture electrons/holes. The captured charges will later be emitted with the time taken before emission determined by the emission time constant of the trap. This process can cause the smearing of the image being recorded, with the smearing caused by the exponential tails from signal charge as it is captured and later released. The dynamics of the capture and release of charge can be described through exponential time constants through Shockley-Read-Hall theory [29,30].

There are several trap species that are known to dominate in the operation of CCDs, Figure 2. In n-channel devices, the traps range from those with shorter emission times, such as the Si-A, through two charge states of the divacancy, to the longer emission time constant of the Si-E. Also included is a trap of unknown origin that is found to exist in various test data in the literature and in mission studies. The energy range for the "unknown" trap may be between 0.30 eV [31] and 0.34 eV [32]. In p-channel devices, three main species are thought to dominate, including a further charge state of the divacancy.
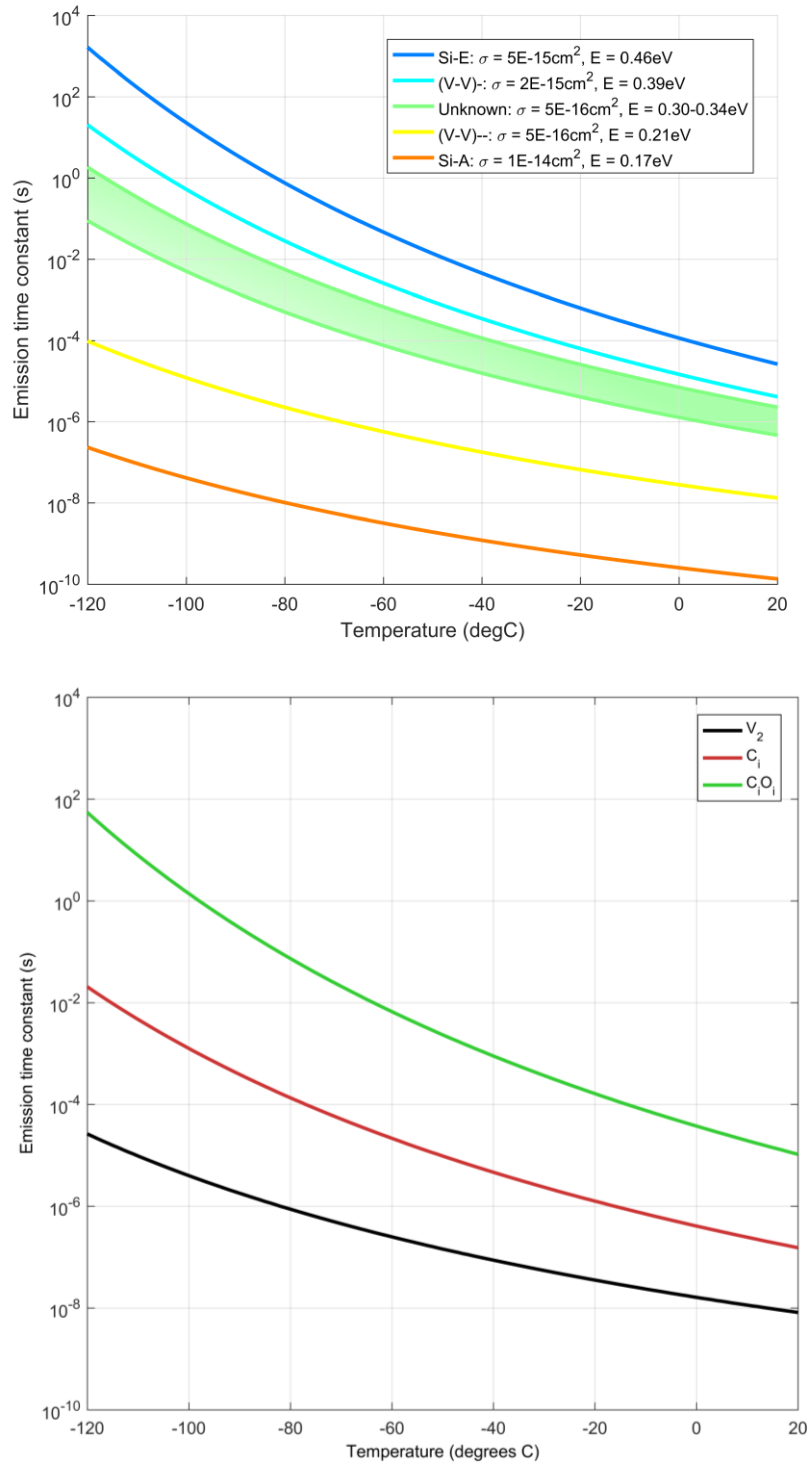
Figure 2. Currently known trap species that are thought to dominate performance degradation in radiation damaged CCDs. *Top*: Electron traps in n-channel devices. The impact of the "unknown" trap species has been noted in a variety of test data, although the exact formation and energy of the trap species is as yet unknown and the subject of further study. *Bottom*: Hole traps in p-channel devices. Plotted from parameters stated in [14].

4. SINGLE TRAP PUMPING TECHNIQUE

Pocket pumping, and the more specific "trap pumping", have been used for over a decade in one form or another to investigate potential pockets and traps within CCDs [12-20]. In this paper, we concentrate on the use of trap pumping to determine precise trap emission time constants and consequently their energy levels and cross-sections. The method used to determine the emission time constant is summarised below, with full details presented in [18].

A flat-field of signal is integrated in the device, either through illumination or another method such as clock-induced charge [33]. If we consider the example of charge stored under phase 1 in a three-phase device as the initial position, the charge can be clocked to phase 2, phase 3, phase 1 in the neighbouring pixel and then back through phase 3, phase 2, and returning to the initial position under phase 1; this denotes one pumping cycle and is repeated (usually for a few thousand cycles). If the charge passes over a trap and an electron is captured then it may be later emitted, either back into the charge packet from which it was captured or into the neighbouring charge packet (it is "pumped") depending on the position of the charge packets at the point of emission. In the presence of a trap, a dipole may therefore be formed, Figure 3. The direction of the dipole (bright-dark or dark-bright) depends on the position of the trap within the pixel (Section 5).

The intensity of the dipole above/below the background can be tracked through repeated operations with different clocking frequencies. Tracing the dipole intensity through images taken with different clock timings allows the generation of something similar to a "resonance curve" for the trap, Figure 4. This data can be fitted with an equation involving only the number of pumps, an analogy to the probability of capture, the dwell time used and the emission time constant of the trap. The exact form of the equation is dependent on the clocking sequence used, with small tweaks allowing the examination of traps in different ways, as discussed in the next section.
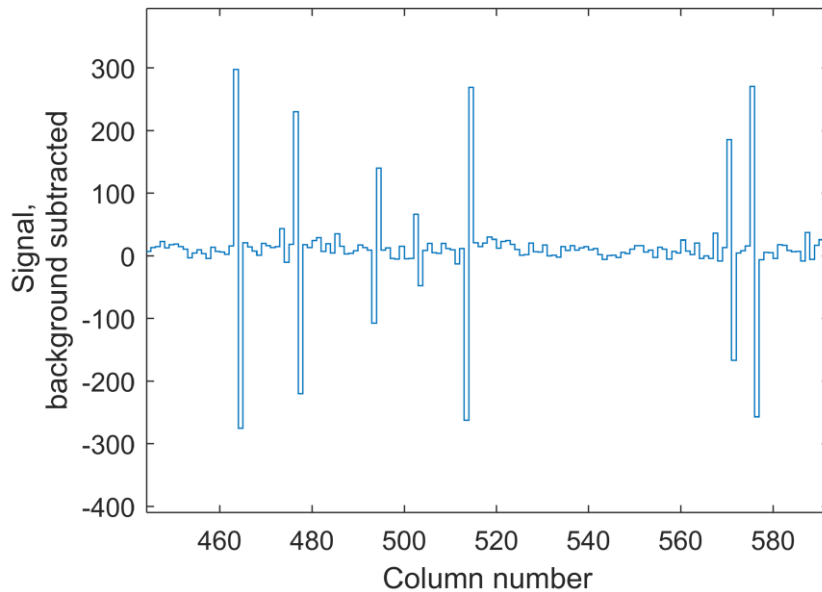
Figure 3. Characteristic dipole features seen in a row profile across the device (with the background signal level subtracted). The dipoles are found with two "directions", light-dark and dark-light; the direction of the dipole enables the location of the trap to be determined to the sub-pixel level (and sub-electrode level for some devices), Section 5. The intensity of the dipoles can be traced with varying clocking frequencies to give a profile similar to that shown in Figure 4.
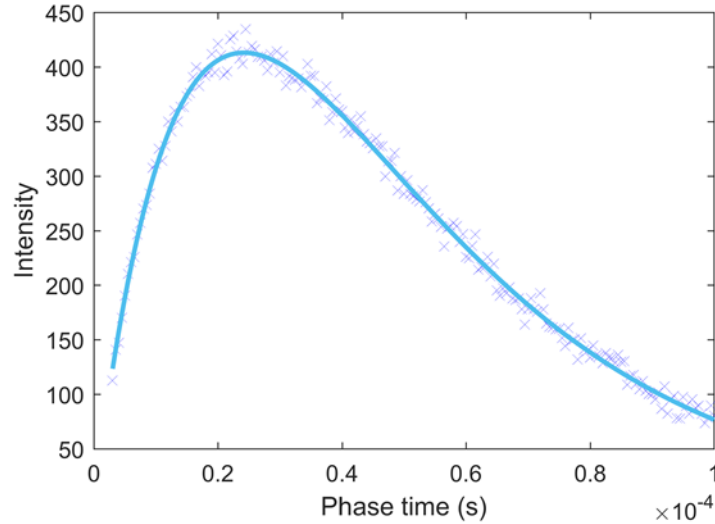
Figure 4. The intensity of a single dipole can be tracked across varying phase times (clock width) to give the data points (crosses) shown. The intensity profile can be fitted with a functional form (solid line) that enables the calculation of the trap emission-time constant and the efficiency of capture.

5. LOCATING THE TRAPS WITHIN THE PIXEL

We can consider the localisation of the traps through the diagrams shown in Figure 5, described here in the context of a four-phase n-channel device. The case of a three-phase device is much simpler than that of the four-phase device and it is usually recommended to operate in a three-phase or pseudo-three-phase mode. However, here we consider a four-phase device to demonstrate the principle of sub-phase location, although a more complex clocking scheme would be required to gain trap parameterisation as detailed in the previous section.

Considering first the top panel: a four-phase device with a trap under phase 2; the signal is integrated under phase 1 and subsequently clocked through phases 2-3-4-1'-4-3-2-1 (where 1' denotes phase 1 in the neighbouring pixel). The trap may capture an electron whilst resting under phase 2, subject to sufficient electron density at the trap position. The time at which the captured electron is emitted, which will depend on the emission time constant of the trap in question, will determine whether the electron is "pumped" into a neighbouring charge packet thus decreasing the signal in the pixel from which it was captured and increasing the signal in the pixel into which it was emitted. Repeating this process leads to the dipoles shown in the previous section.

In Figure 5 (top) the trap will pump signal to the left if the trap is emitted between $2t_{ph}$ and $3t_{ph}$ after capture, leading to a light-dark dipole. In the time periods directly before and after this step, the process is slightly more complicated in a 4-phase device, with the position of the trap under the phase (to the right or left of centre) determining whether the trap pumps or simply releases the electron back into the charge packet from which it captured.

In figure 5 (bottom), we consider the same signal start position and clocking, but now with a trap under phase 3. The time between capture and emission that results in pumping is now different to that in Figure 5 (top). In fact, in this case, only traps to the left-hand-side of phase 3 will pump.

Through symmetry, we can consider traps under phase 2 with a starting position of phase 1 as being identical to traps under phase 3 with a starting position of phase 2. Through combining the dipole positions from various clocking schemes, one can probe not only the phase under which the trap is present, but also under which half of the phase the trap resides.

When a device does not have uniform electrode widths or contains additional doping under one or more phases, the process is again more complex, with AIMO devices for example. Through the use of device simulation software such as ATLAS from SILVACO [34], it is possible to model the potential structure in the pixel and determine the positions under each phase for which pumping would or would not occur for any given clocking scheme.

It is also possible to probe the depth of the trap in the device. Through changing the signal level and clock voltages, the electron density at any fixed trap location in the device can be changed, albeit within limits. Through simulations of charge collection in the device (Section 8), coupled with the measurements of dipole response for the different clock voltages and signal levels, the position of the trap can be estimated within three dimensional space in the device.

6. TRACKING CHANGES IN TRAP POPULATION AND ANNEALLING

The number of a certain species of traps in a device can be seen in the number of dipoles observed when clocking the device at the appropriate "resonant" frequency for the trap species of interest. Results can be repeated with a time period of the order of seconds to track a population of traps through probing at one resonant frequency, Figure 6. In this way, it is possible to investigate a trap species trough formation and annealing in very high levels of detail. New dynamics, such as isothermal annealing at low temperatures, may be observed that can be missed through the use of other analysis techniques.

If a lower time resolution is required, it is possible to "sweep" through a series of clock timings to probe a variety of trap species (if not all species). This process can be looped during irradiation, following irradiation at a set temperature or during a change in temperature. In this way, the dynamics of the trap population can be investigated through time and changes in environment.

7. INVESTIGATING POPULATIONS OF TRAPS

Trap pumping can be used to determine the trap species present through the study of their emission time constants. For each dipole (and therefore each trap) present in the device, the intensity can be tracked for different clocking frequencies and hence the emission time constant found within a few percent accuracy [18-20]. As would be expected, each trap species whilst quoted in the literature with an emission time constant has a distribution of emission time constants, varying from one trap to the next. Through the use of the high time resolution achievable, a distribution of trap emission time constants can be determined within the device, Figure 7. This distribution can be tracked through time, as in Section 6.

Through the investigation of the trap emission time constants it is possible to trace the properties through varying temperature and therefore calculate the trap energy level and cross-section. These additional parameters can be used to determine the likely trap species being investigated, but it should be noted that the trap species can only be implied and not "found" specifically using this method. However, for the purposes of device optimisation and modelling charge transfer through a radiation damaged device it is precisely the emission time constant that is of most importance, not the species. The spread of time constants in Figure 7 is understood to be real and not a measurement uncertainty, with the measurement uncertainty calculated to be of the order of a few percent on each trap.
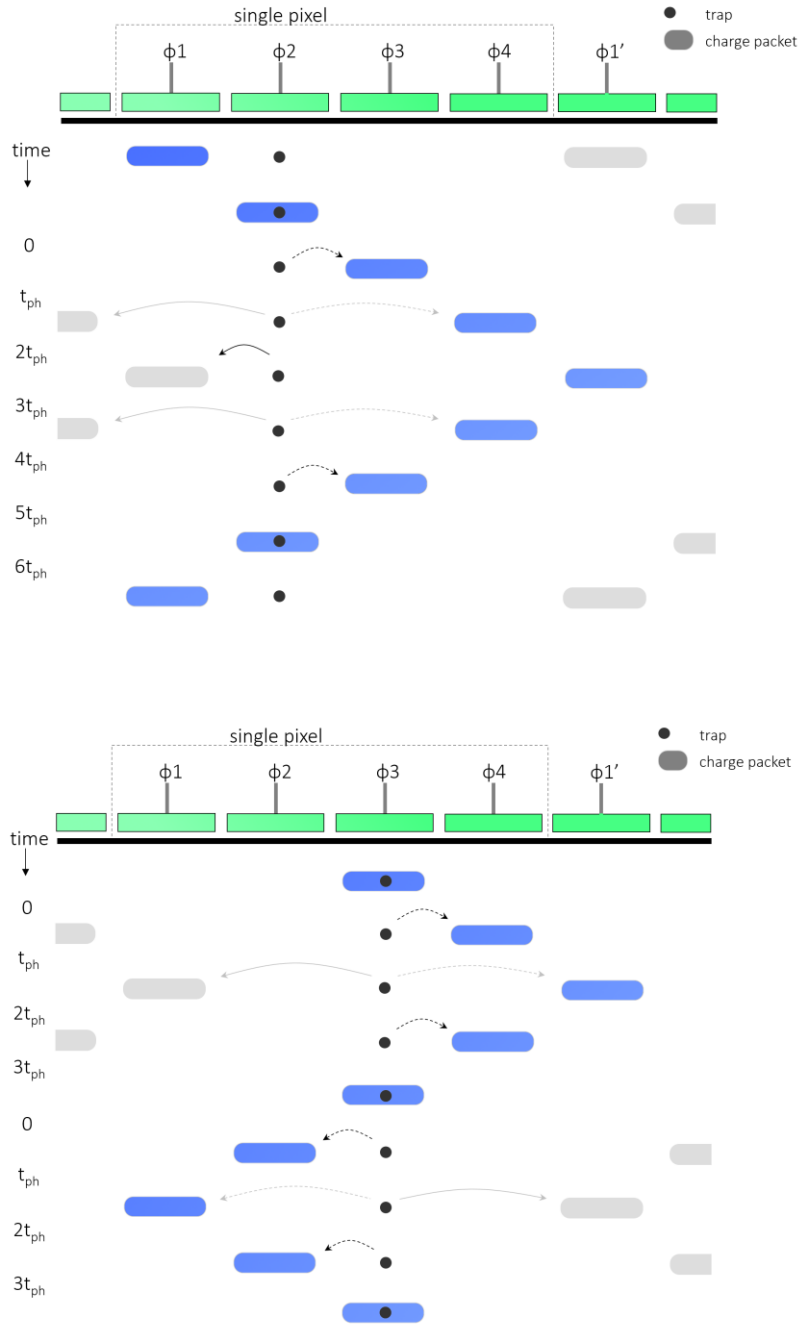
Figure 5. The possibilities for pumping in a four-phase device, showing here two trap locations with the same pumping scheme: a trap under phase 2 (top) and a trap under phase 3 (bottom). A flat field of signal charge is clocked from phase 1 through 2, 3, 4 and into phase 1 in the neighbouring pixel before returning in the reverse direction. The solid arrows denote the positions from which the release of a captured electron (or hole) will result in an increase in the dipole intensity. The dashed arrows denote the positions from which no pumping will occur. In some cases, the location of the trap under the phase will determine whether the trap pumps or not. Using a combination of different clocking schemes, one can probe each possible trap location and determine the trap location to the sub-electrode level.
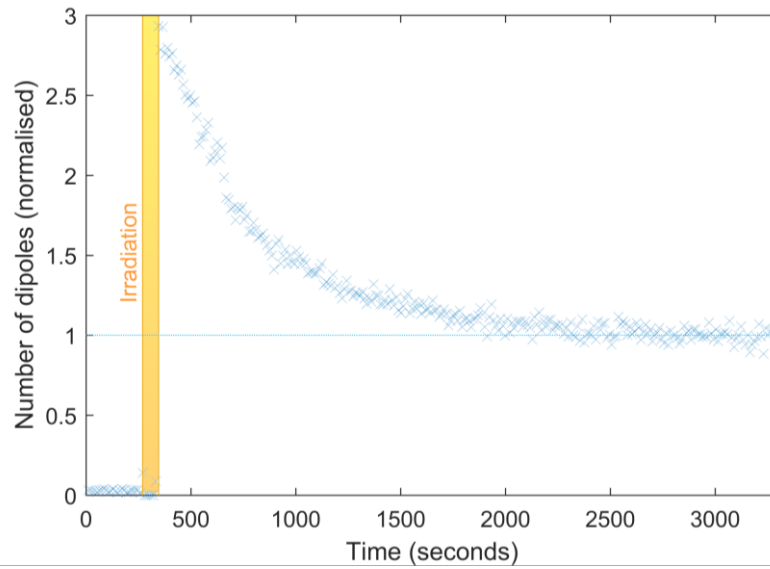
Figure 6. Number of dipoles observed at the expected resonant timing for the double-negative charge state of the divacancy electron trap (Figure 2), normalised to the number of dipoles measured after one hour. The device was maintained at -100˚C throughout testing (including during the irradiation) and measurements taken every approximately 10 seconds. The isothermal annealing observed may be contrary to the expected annealing characteristics of the divacancy at such a low temperature. The trap pumping technique allows measurements to be made with a very high time resolution
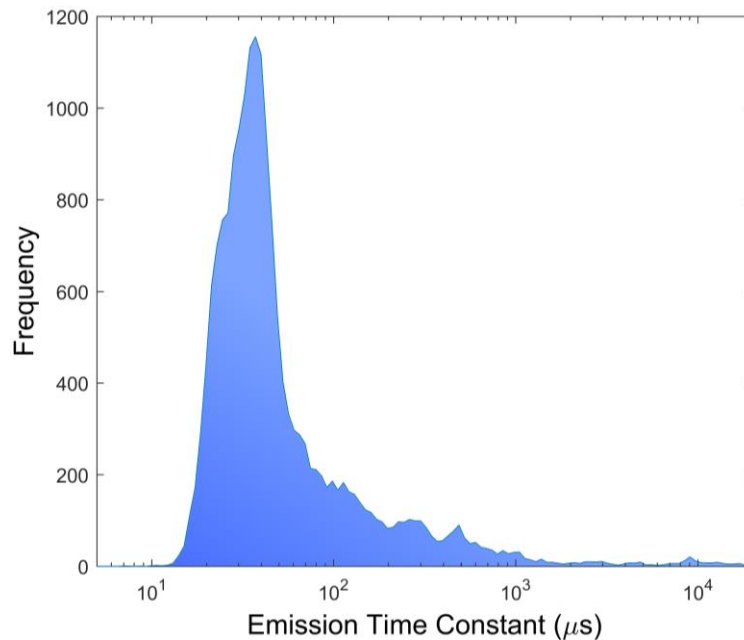
Figure 7. The population of trap species within the device can be probed in great detail. This histogram shows the emission time constants for each individual trap analysed, with the uncertainties assigned to each trap being of the order a few percent. Finer structures are visible, as well as peaks with very low counts across the device. The results shown here are taken from a room temperature irradiation of a p-channel device, tested at 153 K. The main peak is consistent with the expected position of the divacancy hole trap in p-channel devices. Similar analysis can be repeated at regular intervals to examine annealing effects, as well as allowing the comparison of room temperature and cryogenic irradiations. Using such methods, the large difference in trap species produced between room temperature and cryogenic irradiations can be strongly demonstrated.

8. SIMULATING CHARGE TRANSFER

The simulation of charge transfer through a radiation damaged CCD has two main purposes. The first is to understand how images might appear at various stages throughout a mission and to predict performance under changes in experimental conditions. This allows the user to gain a large amount of data without having to carry out the related experiments. However, one must take great care in the use of simulated data as opposed to experimental results. Data taken experimentally under the appropriate conditions should provide results that match what will actually happen during the mission, provided of course that the signal provided is appropriate (e.g. through the use of an illuminated mask of galaxy shapes). Extrapolating from the experimental conditions that have been tested and validated with the simulation should be done with caution, as the validation is only relevant under the experimental conditions tested.

The second use for simulations of charge transfer is in the correction of damaged data, be this through simulating idealised images until the damaged image is achieved or through forward modelling. This is an essential part of gaining the scientific information required from a mission when images are degraded through radiation damage to the detectors as the mission progresses.

There are several, well documented, charge transfer simulations in use currently. The analytical approach has been well used for the Gaia mission [10]. This uses a column-averaged approach and is very effective for the TDI operation of Gaia. An alternative design makes more use of Monte Carlo methods, such as that used for image correction on the Hubble Space Telescope [11].

In recent years, we have developed a full Monte Carlo model at the Open University with the aim of creating a very physical-led simulation of charge transfer in a radiation damaged device. Early results from the model were presented in [35], but the model has recently been redeveloped from the ground-up over the last year [32]. The new Open University Monte Carlo (OUMC) model is fully physics-based and makes use of two new developments.

The SILVACO ATLAS software package enables the simulation of a CCD pixel, from potential structure through to charge storage dynamics [34]. Previous studies of charge storage in a CCD pixel have been shown to be of great use to the Gaia and Euclid CCD studies [36-41]. For the new OUMC [32], we take a three-dimensional simulation of charge storage in a CCD pixel, Figure 8, repeated under each of the appropriate electrode biasing conditions and for a range of charge packet signal sizes. The simulation is sampled at small intervals in all three dimensions and charge density recorded, traced across a large range of signal sizes. In this way, the electron/hole density at any position in the pixel can be interpolated for any signal size. This density is used directly in the simulation to calculate the capture probability, removing the requirement for a parameterised model or approximation. In this way, through the repeated simulation of charge storage in a new device, the simulation should be applicable to any device.
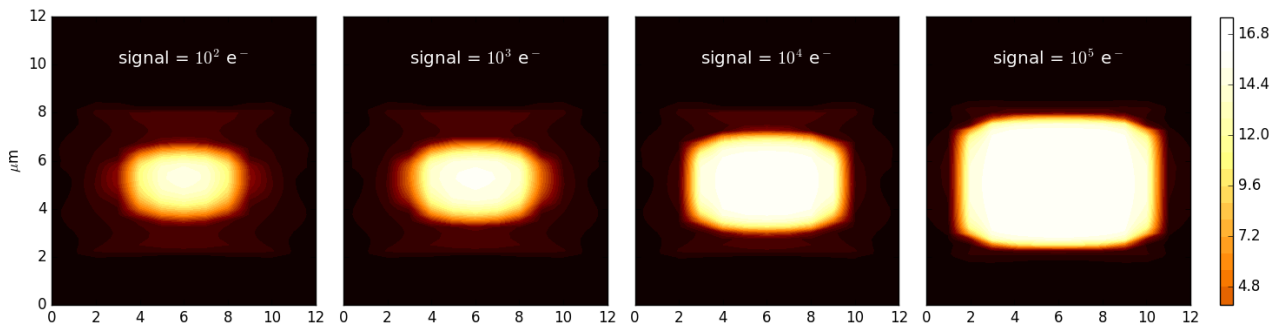
Figure 8. The charge packet is simulated in the Atlas TCAD Silvaco software package for varying signal levels in three dimensions, here showing four "slices" through the 3D charge packet with the charge density shown logarithmically (10^x electrons cm^{-3}). The charge packet can then be sampled over a mesh and incorporated directly into the charge transfer simulation, interpolating for signal levels not directly simulated. In this way, any device can be simulated and implemented in the simulation and giving a physically realistic interpretation of electron (or hole) density within the device.

In addition to providing a more realistic charge density for the capture of charge, an improved implementation of trap emission time constants is also able to be incorporated. The use of trap pumping to determine a histogram of the trap emission time constants across the population of traps allows the traps in the simulation to match those found experimentally in the devices. The study of trap pumping has made it clear that we are far from the situation of having clear and distinct delta-function time constants for each species of trap; instead, we have a continuum of trap emission time constants, Figure 7. Alternative methods to determine trap properties may have flaws that are not immediately apparent. For example, it is common practice to estimate trap emission time constants from fits to charge tails. This may not give accurate trap parameters as there is no inclusion in this method of recapture and emission from the charge tails; an issue that has been highlighted through testing with the simulation detailed in [32].

9. SUMMARY

The trap pumping technique has been shown over recent years to be a powerful tool to analyse the properties of traps within CCDs. Following irradiation, be that in space during a mission or in the laboratory in pre-launch testing, knowledge of the trap parameters, such as the emission time constant, is essential for aiding in optimisation of device operation and for image correction techniques. The use of trap pumping to determine precise trap properties and dynamics also has the potential to aid the possible future development of more radiation hard detectors through defect engineering [42-44].

Through trap pumping with a carefully chosen selection of clocking schemes, traps can be located to the sub-electrode level. Each of these traps can be traced in temperature and time to find the energy level of that specific trap and the cross-section. The distribution of the population of trap emission time constants combined can be used directly in charge transfer simulations that, with the direct implementation of Silvaco-driven charge density distributions, allow a more physical interpretation of the capture and emission of charge by traps; no approximations of spread or number density are required.

10. ACKNOWLEDGEMENTS

REFERENCES

[1] M. J. L. Turner, A. Abbey, M. Arnaud, M. Balaini, M. Barbera, E. Belole, P. J. Bennie, J. P. Bernard, G. F. Bignami, M. Boer, U. Briel, I. Butler, C. Cara, C. Chabaud, R. Cole, A. Collura, M. Conte, A. Cros, M. Denby, P. Dhez, G. Di Coco, J. on, P. Ferrando, S. Ghizzardi, F. Gianotti, C. V. Goodall, L. Gretton, R. G. Griffiths, O. Hainaut, J. F. Hochedez, A. D. Holland, E. Jourdain, E. Kendziorra, A. Lago tina, R. Laine, N. La Palombara, M. Lortholary, D. Lumb, P. Marty, S. Molendi, C. Pigot, E. Poindron, K. A. Pounds, J. N. Reeves, C. Reppin, R. Rothenflug, P. Salvetat, J. L. Sauvageot, D. Schmitt, S. Sembay, A. D. T. Short, J. Spragg, J. Stephen, L. Strüder, A. Tiengo, M. Trifoglio, J. Trümper, S. Vercellone, L. Vigroux, G. Villa, M. J. Ward, S. Whitehead and E. Zonca, "The European Photon Imaging Camera on XMM-Newton: The MOS cameras", A&A, 365 1 (2001) L27-L35

[2] L. Lindegren, C. Babusiaux, C. Bailer-Jones, U. Bastian, A. G. A. Brown, M. Cropper, E. Hg, C. Jordi, D. Katz, F. van Leeuwen, X. Luri, F. Mignard, J. H. J. de Bruijne and T. Prusti, "The Gaia mission: science, organization and present status", IAU Colloq., vol. 248, pp. 217-223, Jul. 2008.

[3] Katz, D.; Cropper, M.; Meynadier, F.; Jean-Antoine, A.; Allende Prieto, C.; Baker, S.; Benson, K.; Berthier, J.; Bigot, L.; Blomme, R.; Boudreault, S.; Chemin, L.; Crifo, F.; Damerdji, Y.; David, M.; David, P.; Delle Luche, C.; Dolding, C.; Frémat, Y.; Gerbier, N.; Gerssen, J.; Gómez, A.; Gosset, E.; Guerrier, A.; Guy, L.; Hall, D.; Hestroffer, D.; Huckle, H.; Jasniewicz, G.; Ludwig, H-G.; Martayan, C.; Morel, T.; Nguyen, A.-T.; Ocvirk, P.; Parr, C.; Royer, F.; Sartoretti, P.; Seabroke, G.; Simon, E.; Smith, M.; Soubiran, C.; Steinmetz, M.; Thévenin, F.; Turon, C.; Udry, S.; Veltz, L. and Viala, Y. (2010). Gaia spectroscopy: processing, performances and scientific returns. EAS Publications Series, 45 pp. 189–194.

[4]   R. Laureijs, et al. (2011, Oct). Euclid Definition Study Report, ArXiv e-prints 1110.3193 [Online]. Available: http://arxiv.org/abs/1110.3193.

[5]   Cropper, Mark; Pottinger, S.; Niemi, S.-M.; Denniston, J.; Cole, R.; Szafraniec, M.; Mellier, Y.; Berthé, M.; Martignac, J.; Cara, C.; di Giorgio, A. M.; Sciortino, A.; Paltani, S.; Genolet, L.; Fourmand, J.-J.; Charra, M.; Guttridge, P.; Winter, B.; Endicott, J.; Holland, A.; Gow, J.; Murray, N.; Hall, D.; Amiaux, J.; Laureijs, R.; Racca, G.; Salvignol, J.-C.; Short, A.; Lorenzo Alvarez, J.; Kitching, T.; Hoekstra, H. and Massey, R. (2014). VIS: the visible imager for Euclid. In: Space Telescopes and Instrumentation 2014: Optical, Infrared, and Millimeter Wave, 22-27 July 2014, Montréal, Quebec.

[6]   M. Cropper; S. Pottinger; S.-M. Niemi; J. Denniston; R. Cole; M. Szafraniec; Y. Mellier; M. Berthé; J. Martignac; C. Cara; A. M. di Giorgio; A. Sciortino; S. Paltani; L. Genolet; J.-J. Fourmand; M. Charra; P. Guttridge; B. Winter; J. Endicott; A. Holland; J. Gow; N. Murray; D. Hall; J. Amiaux; R. Laureijs; G. Racca; J.-C. Salvignol; A. Short; J. Lorenzo Alvarez; T. Kitching; H. Hoekstra; R. Massey, "VIS: the visible imager for Euclid", Proc. SPIE 9143, Space Telescopes and Instrumentation 2014: Optical, Infrared, and Millimeter Wave, 91430J (2 August 2014).

[7]   Short, A. D.; Barry, D.; Berthe, M.; Boudin, N.; Boulade, O.; Cole, R.; Cropper, M.; Duvet, L.; Endicott, J.; Gaspar Venancio, L.; Gow, J.; Guttridge, P.; Hall, D.; Holland, A.; Israel, H.; Kohley, R.; Laureijs, R.; Lorenzo Alvarez, J.; Martignac, J.; Maskell, J.; Massey, R.; Murray, N.; Niemi, S.-M.; Pool, P.; Pottinger, S.; Prod'homme, T.; Racca, G.; Salvignol, J-C; Suske, W.; Szafraniec, M.; Verhoeve, P.; Walton, D. and Wheeler, R. (2014). The Euclid VIS CCD detector design, development, and programme status. In: High Energy, Optical, and Infrared Detectors for Astronomy VI, 22-27 June 2014, Montréal, Quebec.

[8]   Gow, J. P. D.; Murray, Neil; Holland, Andrew; Hall, D. J. Hall; Cropper, M.; Hopkinson, G. and Duvet, L. (2012). "Assessment of space proton radiation-induced charge transfer inefficiency in the CCD204 for the Euclid space observatory". Journal of Instrumentation, 7 (C01030).

[9]   Gow, J. P. D.; Murray, N. J.; Hall, D. J.; Clarke, A. S.; Burt, D.; Endicott, J. and Holland, A. D. (2012). "Assessment of proton radiation-induced charge transfer inefficiency in the CCD273 detector for the Euclid Dark Energy Mission". In: High Energy, Optical, and Infrared Detectors for Astronomy V, 1-6 July 2012, Amsterdam.

[10]   A. Short, C. Crowley, J.H.J. de Bruijne and T. Prod'homme, "An analytical model of radiation-induced charge transfer inefficiency for CCD detectors", MNRAS, vol. 430, no. 4, pp. 3078-3085, Apr. 2013.

[11]   Massey, Richard; Schrabback, Tim; Cordes, Oliver; Marggraf, Ole; Miller, Lance; Hall, David; Cropper, Mark; Prod'homme, Thibaut and Matias Niemi, Sami (2014). "An improved model of charge transfer inefficiency and correction algorithm for the Hubble Space Telescope". Monthly Notices of the Royal Astronomical Society, 439(1) pp. 887–907.

[12]   J. R. Janesick, "Charge transfer" in Scientific charge-coupled devices, Washington: SPIE - The International Society for Optical Engineering, 2001.

[13]   R. Kohley ; F. Raison ; J. M. Martin-Fleitas; Gaia: operational aspects and tests of Gaia Flight Model CCDs. Proc. SPIE 7439, Astronomical and Space Optical Systems, 74390F (September 17, 2009).

[14]   Nick J. Mostek ; Christopher J. Bebek ; Armin Karcher ; William F. Kolbe ; Natalie A. Roe ; Jonathan Thacker; "Charge trap identification for proton-irradiated p+ channel CCDs". Proc. SPIE 7742, High Energy, Optical, and Infrared Detectors for Astronomy IV, 774216 (July 16, 2010).

[15]   Murray, N. J.; Holland, A. D.; Gow, J. P. D.; Hall, D. J.; Tutt, James H.; Burt, D. and Endicott, J. (2012). "Mitigating radiation-induced charge transfer inefficiency in full-frame CCD applications by 'pumping' traps". In: High Energy, Optical, and Infrared Detectors for Astronomy V, 1-6th July 2012, Amsterdam.

[16]   Murray, Neil J.; Burt, David J.; Hall, David and Holland, Andrew D. (2013). "The relationship between pumped traps and signal loss in buried channel CCDs". In: UV/Optical/IR Space Telescopes and Instruments: Innovative Technologies and Concepts VI,, 25-26 August 2013, San Diego, SPIE.

[17]   Hall, David; Gow, Jason; Murray, Neil and Holland, Andrew (2012). "Optimisation of device clocking schemes to minimise the effects of radiation damage in charge-coupled devices". IEEE Transactions on Electron Devices, 59(4) pp. 1099–1106.

[18]   Hall, David J.; Murray, Neil J.; Holland, Andrew D.; Gow, Jason; Clarke, Andrew and Burt, David (2014). Determination of in situ trap properties in CCDs using a "single-trap pumping" technique. IEEE Transactions on Nuclear Science, 61(4) pp. 1826–1833.

[19]   Hall, David J.; Murray, Neil; Gow, Jason; Wood, Daniel and Holland, Andrew (2014). "In situ trap parameter studies in CCDs for space applications". In: High Energy, Optical, and Infrared Detectors for Astronomy VI, 22-27 June 2014, Montréal, Quebec, p. 915408.

[20] Wood, D.; Hall, D.; Murray, N.; Gow, J. and Holland, A. (2014). "Studying charge-trapping defects within the silicon lattice of a p-channel CCD using a single-trap "pumping" technique". Journal of Instrumentation, 9, article no. C12028.

[21] Murray, Neil J.; Holland, Andrew D.; Gow, Jason P. D.; Hall, David J.; Stefanov, Konstantin D.; Dryer, Ben J.; Barber, Simeon and Burt, David J. (2014). "Assessment of the performance and radiation damage effects under cryogenic temperatures of a P-channel CCD204s". In: High Energy, Optical, and Infrared Detectors for Astronomy VI, 22-27 July 2014, Montréal, Quebec.

[22] Gow, J. P. D.; Smith, P. H.; Pool, P.; Hall, D. J.; Holland, A. D. and Murray, N. J. (2015). "Proton irradiation of a swept charge device at cryogenic temperature and the subsequent annealing". Journal of Instrumentation, 10(1), article no. C01037.

[23] Gow, J. P. D.; Wood, D.; Burt, D.; Hall, D. J.; Dryer, B. J.; Holland, A. D. and Murray, N. J. (2015). Initial results from a cryogenic proton irradiation of a p-channel CCD. In: UV, X-Ray, and Gamma-Ray Space Instrumentation for Astronomy XIX, article no. 96010F.

[24] Harding, Leon K.; Demers, Richard T.; Hoenk, Michael; Peddada, Pavani; Nemati, Bijan; Cherng, Michael; Michaels, Darren; Neat, Leo S.; Loc, Anthony; Bush, Nathan; Hall, David; Murray, Neil; Gow, Jason; Burgon, Ross; Holland, Andrew; Reinheimer, Alice; Jorden, Paul R. and Jordan, Douglas (2015). Technology advancement of the CCD201-20 EMCCD for the WFIRST coronagraph instrument: sensor characterization and radiation damage. Journal of Astronomical Telescopes, Instruments, and Systems, 2(1) 011007.

[25] Harding, Leon K.; Demers, Richard T.; Hoenk, Michael; Peddada, Pavani; Nemati, Bijan; Cherng, Michael; Michaels, Darren; Loc, Anthony; Bush, Nathan; Hall, David; Murray, Neil; Gow, Jason; Burgon, Ross; Holland, Andrew; Reinheimer, Alice; Jorden, Paul R. and Jordan, Douglas (2015). Electron multiplication CCD detector technology advancement for the WFIRST-AFTA coronagraph. In: Techniques and Instrumentation for Detection of Exoplanets VII (Shaklan, Stuart ed.), Proceedings of SPIE, SPIE Press, article no. 96050F.

[26] Hall, David J.; Bush, Nathan; Murray, Neil; Gow, Jason; Clarke, Andrew; Burgon, Ross and Holland, Andrew (2015). Challenges in photon-starved space astronomy in a harsh radiation environment using CCDs. In: Proceedings of SPIE, Society of Photo-Optical Instrumentation Engineers (SPIE), 9602, article no. 96020U.

[27] Bush, Nathan; Hall, David; Holland, Andrew; Burgon, Ross; Murray, Neil; Gow, Jason; Soman, Matthew; Jordan, Doug; Demers, Richard; Harding, Leon K.; Hoenk, Michael; Michaels, Darren; Nemati, Bijan and Peddada, Pavani (2015). The impact of radiation damage on photon counting with an EMCCD for the WFIRST-AFTA coronagraph. In: Proceedings of SPIE, Society of Photo-Optical Instrumentation Engineers (SPIE), 9605, article no. 96050E.

[28] Srour J. R., Marshall C.J., and Marshall P.W. (2003) "Review of Displacement Damage Effects in Silicon Devices", IEEE Trans. Nucl. Sci., vol. 50, Issue 3.

[29] W. Shockley and W. T. Read Jr., "Statistics of the recombinations of holes and electrons", Phys. Rev., vol. 87, no. 5, pp. 835-842, Sept. 1952.

[30] R. N. Hall, "Electron-hole recombination in germanium", Phys. Rev., vol. 87, no. 5, pp. 387-387, Jul. 1952.

[31] Holland, A.; Abbey, A.; Lumb, D.; McCarthy, K., "Proton damage effects in EEV charge coupled devices", EUV, X-ray, and Gamma-ray instrumentation for astronomy; Proceedings of the Meeting, San Diego, CA, July 11-13, 1990 (A92-20226 06-35). Bellingham, WA, Society of Photo-Optical Instrumentation Engineers, 1990, p. 378-395

[32] Jesper Skottfelt, David Hall, Jason Gow, Neil Murray, Andrew Holland, and Thibaut Prod'homme, (2016) "Comparing simulations and test data of a radiation damaged CCD for the Euclid mission", Proc SPIE Astronomical Telescopes and Instrumentation, High Energy, Optical, and Infrared Detectors for Astronomy VII, 9915-83 (In Press).

[33] Murray, Neil J.; Burt, David J.; Holland, Andrew D.; Stefanov, Konstantin D.; Gow, Jason P. D.; MacCormick, Calum; Dryer, Ben J. and Allanwood, Edgar A. H. (2013). Multi-level parallel clocking of CCDs for: improving charge transfer efficiency, clearing persistence, clocked anti-blooming, and generating low-noise backgrounds for pumping. In: UV/Optical/IR Space Telescopes and Instruments: Innovative Technologies and Concepts VI, SPIE, article no. 8860-20.

[34] ATLAS User's Manual, "Device simulation software", SILVACO Inc., 20th April 2010.

[35] Hall, David J.; Holland, Andrew; Murray, Neil; Gow, Jason and Clarke, Andrew (2012). "Modelling charge transfer in a radiation damaged charge coupled device for Euclid". In: High Energy, Optical, and Infrared Detectors for Astronomy V, 01-06 July 2012, Amsterdam.

[36] Seabroke, G., Holland, A., Cropper, M., "Modelling radiation damage to ESA's Gaia satellite CCDs",Proc. SPIE, 7021 (2008).

[37]   Seabroke, G., Holland, A., Burt D., Robbins, M., "Modelling electron distributions within ESA's Gaia satellite CCD pixels to mitigate radiation damage", Proc. SPIE, 7439 (2009)

[38]   G. M. Seabroke, A. D. Holland, D. Burt, M. S. Robbins, "Silvaco ATLAS model of ESA's Gaia satellite e2v CCD91-72 pixels", Proc. of SPIE Astronomical Telescopes and Instrumentation (High Energy, Optical, and Infrared Detectors for Astronomy IV), 27-30 June 2010, San Diego, USA

[39]   Clarke, A. S.; Hall, D. J.; Holland, A. and Burt, D. (2012). "Modelling charge storage in Euclid CCD structures". Journal of Instrumentation, 7 (C0105)

[40]   Clarke, A.; Hall, D.; Murray, N.; Holland, A. and Burt, D. (2012). "Device modelling and model verification for the Euclid CCD273 detector". In: High Energy, Optical, and Infrared Detectors for Astronomy V, 1-6th July 2012, Amsterdam.

[41]   Clarke, A.; Hall, D.; Murray, N.; Gow, J.; Holland, A. and Burt, D. (2013). "Pixel-level modelling and verification for the EUCLID VIS CCD". In: UV/Optical/IR Space Telescopes and Instruments: Innovative Technologies and Concepts VI, 25-26 August 2013, San Diego, SPIE.

[42]   Londos, C. A.; Sgourou, E. N.; Hall, D. and Chroneos, A. (2014). "Vacancy-oxygen defects in silicon: the impact of isovalent doping". Journal of Materials Science: Materials in Electronics, 25(6) pp. 2395–2410.

[43]   Wang, Hao; Chroneos, Alexander; Hall, David; Sgourou, Efi and Schwingenschlogl, Udo (2013). Phosphorous-vacancy-oxygen defects in silicon. Journal of Materials Chemistry A, 1(37) pp. 11384–11388.

[44]   H. Wang, A. Chroneos, C. A. Londos, E. N. Sgourou, and U. Schwingenschlögl, "A-centres in silicon studied with hybrid density functional theory", Appl. Phys. Lett. 103, 052101 (2013).